

# Simulation and Modeling of a Photovoltaic Pumping Installation by Bond Graph

Hamdouni Belgacem\*, Riahi Jamel, Dhafer Mezghanni and Mami Abdelkader

Laboratory for the Application of Energy Efficiency and Renewable Energies, FST, Tunis, Tunisia; Belgacem.hamdouni@fst.utm.tn, Riahijamel100@gmail.com, dhafer.mezghanni@gmail.com, mami.abdelkader@planet.tn

## Abstract

**Objectives:** To model and simulate the pumping system by using as a source the PV and by the vectorial and scalar commands. **Methods:** The photovoltaic system modelling is complex; so we propose the use of bond graph (BG) methodology which permits the decomposition of the system into subsystems exchanging energy, and to represent several physic domains (electricity, mechanical, etc.) with an joined way. **Findings:** We represent a method based on the input-output causal inversion of the bond graph of the system which consists in deducing the laws from input-output control directly on bond graph. A new technique that consists on using a PWM bloc with three phases inverters is employed in order to optimize this bloc and to have better results. **Applications:** The modeling of photovoltaic system elements is an important step that should be preceded all application of sizing, identification or simulation.

**Keywords:** Bond Graph Modeling, Induction Motor, MPPT, Photovoltaic, PWM, Scalar and Vector Control

## 1. Introduction

Photovoltaic is considered as the most direct way to convert solar radiation into electricity; Solar PV generates no pollution. The direct conversion of sunlight to electricity occurs without any moving parts. This method of energy conversion has some advantages like: modular construction, flexibility of use, short installation and operation time and high regularity and low maintenance.<sup>1,3</sup>

It is known that the PV system modeling is the most complicated system. For this reason, we suggest a very useful method: the bond graph in which we can separate the principal system into parts (subsystems) in order to exchange the energy and to unify the different domains.

We will present the optimization of the PWM bloc by applying the vector command of the  $\alpha\beta$  motor and other tasks will also be used. The photovoltaic system we used in this work is built by a PV, a CC-CC, a CC-AC and a Motor-pump as presented in Figure 1.

A photovoltaic cell is a special finite energy source of non-linear current-voltage characteristic.

The photovoltaic generator behavior is equivalent to a shunted current source by a junction diode D and identical to it. The relation current-voltage of the photovoltaic diode is also non-linear.<sup>1,9</sup>

In order to maintain the different physical phenomena at the photopile level, such as contact resistances, leakage current by the boards and ancient cells, the model is supplemented by two series of resistors:  $R_{s0}$  and shunt  $R_{sh0}$  as represented in the following Figure 2.

The current-voltage characteristic of the photovoltaic cell is given by the following equation:

$$I_i = I_{phi} - I_{SSi} \left( \exp \left( \frac{V_i + R_{si} I_i}{V_{Ti}} \right) - 1 \right) - \frac{V_i + R_{si} I_i}{R_{shi}} \quad (I-1)$$

\*Author for correspondence

With

- $I_{phi}$  is the photo-current of the cell, under standard conditions the current corresponds to the short-circuit current.
- $I_{ssi}$  is the inverse current of the diode, depends on the temperature of the junction  $T_p$ ,
- $I_d$  is the current passing through the diode.
- $V_{Ti}$  is the thermodynamic potential given by  $\frac{n_i K T_p}{q}$
- The photovoltaic power of the cell type  $P_i$ , produced by the current  $I_i$  and the voltage  $V_i$ , is represented by the nonlinear characteristic  $P_i(V_i)$  and the characteristic  $I_i(V_i)$  given in Figure 3.

### 1. Bond graph modeling of the photovoltaic generator:

There are many applications of the generator especially in isolated areas (mountain huts, small telecommunication relays, measurement stations, road signs ...) or mobile residence (pleasure boats, caravans ...).

In order to introduce the association of electric machines to the photovoltaic generator, we treat in the first step a standard equivalent circuit of a PV source coupled to a load  $R_L$  represented in Figure 4. In the other hand we model the diode by a nonlinear resistor whose current-voltage relation is indicated by a nonlinear function  $\psi_{RD}$ .

Subsequently, we pass to a simplification phase of the model which consist to neglect the different effect of the resistances  $R_{sh}$  and  $R_s$  (which is also justified the orders of the magnitudes of the resistances). Figure 5a and 5b represents respectively the reduced equivalent circuit of a PV source with starting up capacity and its model BG<sup>1</sup>.

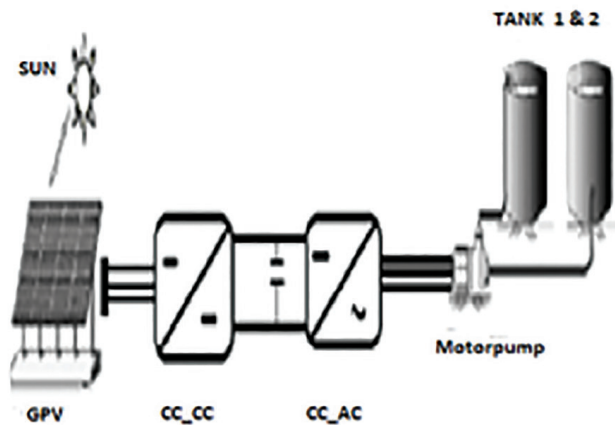


Figure 1. Schematic diagram of the photovoltaic structure.

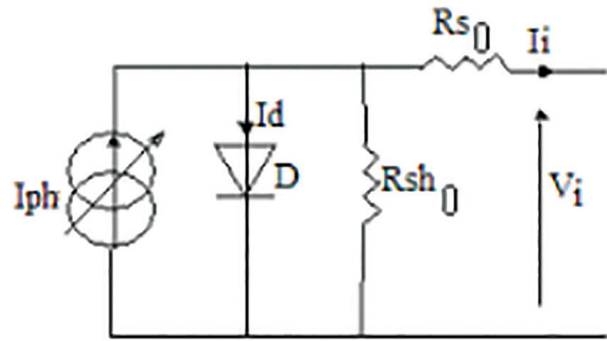


Figure 2. Equivalent electrical diagram of a PV cell.

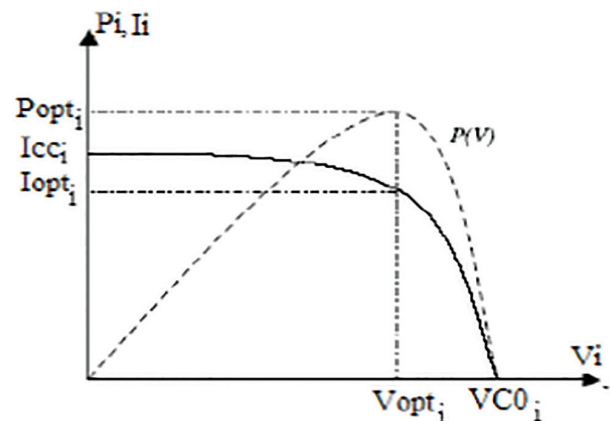


Figure 3. Characteristic current-voltage and power-voltage Of a photovoltaic cell.

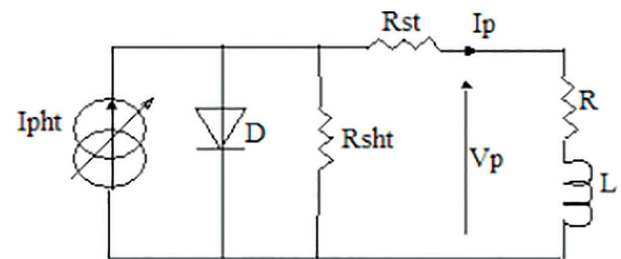


Figure 4. Equivalent system of a PV generator coupled to an R-L load.

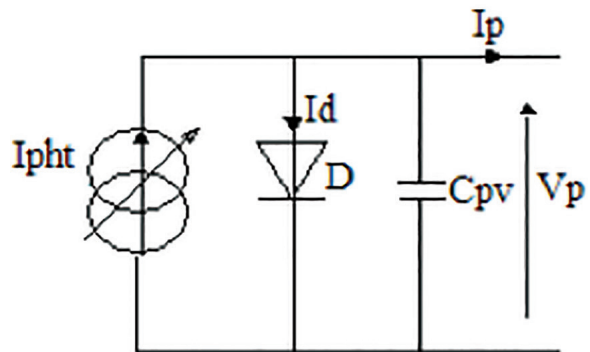


Figure 5a. GPV circuit diagram with starting-up capacity.

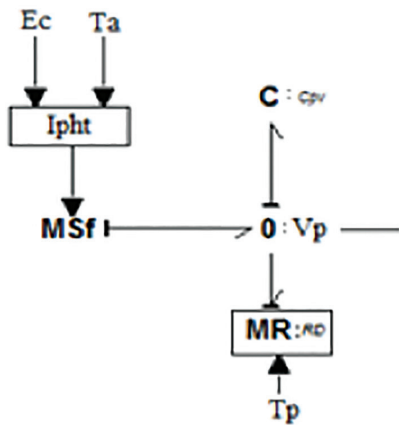


Figure 5b. A bond graph model reduced of a PV generator.

## 2. Modeling of the CC / CC converter

A chopper circuit is used to refer to numerous types of electronic switching devices and circuits used in power control and signal applications. A chopper is a CC / CC (continuous/continuous) converter; it permits to obtain an adaptable continuous voltage from a fixed continuous voltage.

Either in a photovoltaic structure using a buck chopper whose output voltage  $V_c$  is lower than its input voltage  $V_p$  delivered by the PV generator Figure 6.

To obtain the average medium bond graph model in Figure 7, a model construction procedure has been developed and manipulated by<sup>2</sup>

This procedure consists of six steps, the details of which are not part of our study; it has led to the bond graph model, given by Figure 7.

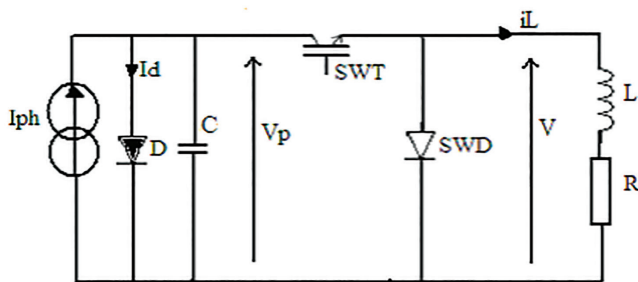


Figure 6. Circuit diagram of the PV system With a buck chopper.

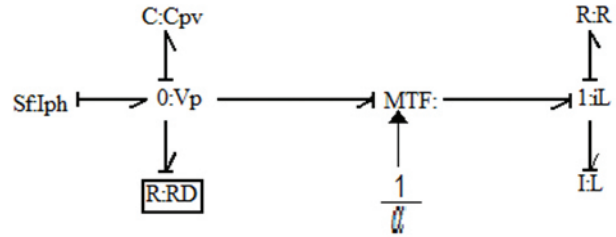


Figure 7. Medium bond graph model of a PV structure+ devolter chopper + load R-L.

## 2. Search for Maximum Power Point

Maximum power point tracking is a technique used commonly with wind turbines and photovoltaic (PV) solar systems to maximize power extraction under all conditions.

Although solar power is mainly covered, the principle applies generally to sources with variable power: for example, optical power transmission and thermophotovoltaics.

To convert the available energy to a continuous one with the best efficiency, it is fundamental to work with an optimum operating point, which corresponds to the maximum power provided by the PV generator. That is possible by constantly adapting the generator to its load due to a converter which plays the role of adapted impedance. This procedure is known as a technique for continuation of the point of maximum power or MPPT.

### 2.1 Search for the maximum power point for PV generator

The maximum power point is usually controlled by two control variables: The voltage or the power, which are measured each time and used again in a loop to determine the maximum power point. The perturbation and observation method (P & O) is used in photovoltaic applications. The implementation of MPPT between PV generator and chopper is given in Figure 8.<sup>3,6,7</sup>

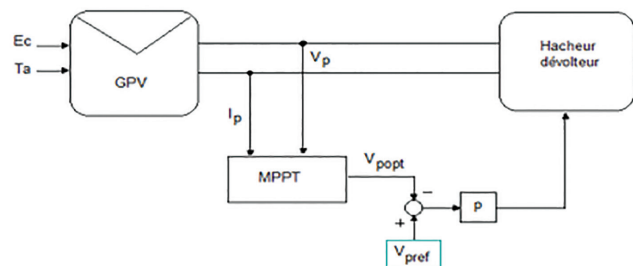


Figure 8. Control diagram of the chopper.

## 2.2 Perturbation and observation method (P & O)

The 'P & O' perturbation and observation method is the most widespread in the Industrial, because its algorithm is easy to implement. This process Disturbance of the system by increasing or decreasing the operating voltage of the module and observe its effect on the output power of the row.

According to<sup>8</sup>: The perturbation and observation method is an extensively approach used to MPPT research view it is simplicity and it requires only voltage measurements and photovoltaic panel current  $V_{pv}$  and  $I_{pv}$  respectively. It can deduce the point of maximum power even during variations of illumination and temperature.

## 2.3 Modeling of the CC / AC converter

CC / AC converter permit the continuous-alternative conversion; it is about the voltage inverter represented in Figure 9. It is controlled by a symmetrical regular sampling pulse width modulation strategy enabling, at each switching period, to give a variable average supply voltage across the motor.

We consider the case where the inverter is ideal and its switches are perfect and switch instantly. The bond graph model is deduced via the relations describing the operation of the three arms of the inverter. In fact, according to the diagram in figure 9, the voltage  $v_{1o}$  is  $U_c / 2$  when the switch T1 is on and the switch T4 is off, it changes sign when T4 is on and T1 is off. The same reasoning is available for  $v_{2o}$  using the switches T2 and T5 and on the other hand for  $v_{3o}$  by using the switches T3 and T6 and by associating with the switches  $T_i$  the control signals  $C_{iref}$  like  $C_{iref} = 1$  when the switch  $T_i$  is on and  $C_{iref} = 0$  when  $T_i$  is blocked, then we can write the following equations:

$$\begin{aligned} v_{1o} &= (C_{1ref} - C_{4ref}) U_c / 2 \\ v_{2o} &= (C_{2ref} - C_{5ref}) U_c / 2 \\ v_{3o} &= (C_{3ref} - C_{6ref}) U_c / 2 \end{aligned} \quad (I-2)$$

The different voltages composants (voltage between two phases) are expressed by:

$$\begin{aligned} u_{12} &= v_{1o} - v_{2o} = (C_{1ref} - C_{4ref} - C_{2ref} + C_{5ref}) U_c / 2 \\ u_{23} &= v_{2o} - v_{3o} = (C_{2ref} - C_{5ref} - C_{3ref} + C_{6ref}) U_c / 2 \\ u_{31} &= v_{3o} - v_{1o} = (C_{3ref} - C_{1ref} - C_{6ref} + C_{4ref}) U_c / 2 \end{aligned} \quad (I-3)$$

The simpl voltages  $v_{s1}$ ,  $v_{s2}$  and  $v_{s3}$  are connected to the compound voltages  $u_{12}$ ,  $u_{31}$  by:

$$u_{12} = v_{s1} - v_{s2} \quad (I-4)$$

$$u_{31} = v_{s3} - v_{s1} \quad (I-5)$$

Then:

$$U_{12} - u_{31} = 2 v_{s1} - v_{s2} - v_{s3} \quad (I-6)$$

In the case of a balanced three-phase load we verify by the following equation:

$$v_{s1} + v_{s2} + v_{s3} = 0 \quad (I-7)$$

By involving the preceding relations, we should have in matrix writing:

$$\begin{bmatrix} v_{s1} \\ v_{s2} \\ v_{s3} \end{bmatrix} = \frac{U_c}{6} \begin{pmatrix} 2 & -1 & -1 \\ -1 & 2 & -1 \\ -1 & -1 & 2 \end{pmatrix} \begin{bmatrix} C_{1ref} - C_{4ref} \\ C_{2ref} - C_{5ref} \\ C_{3ref} - C_{6ref} \end{bmatrix} \quad (I-8)$$

Referring to the relationship I-8, the sub model bond graph of an arm of the inverter (Arm A) given in Figure 10.

The model given by Figure 10 represents a "sub-model" of a multi-command MTF element modeling an inverter arm and controlled by the vector

$$\zeta = [C_{1ref}, C_{2ref}, C_{3ref}, C_{4ref}, C_{5ref}, C_{6ref}]^T.$$

The BG model of an arm of the inverter is given by Figure 11.

With a Similar way, we model the two other arms B and C of the voltage inverter. In Figure 12 we represent the bond graph model of the three-phase voltage inverter as well as the control of its arms.

We suppose that the blocking of the switch  $T_i$  and the switching on of the switch  $T_{3+i}$  happen at the same time, with this hypothesis we can write the following relation:

$$C_{i+1ref} = 1 - C_{iref} \quad ; i \in \{1, 2, 3\} \quad \forall t \quad (I-9)$$

It is verified that the mean value of the PWM wave takes the form of a sinusoid, it's the modulating wave. In practice, the blocking of the switch  $T_i$  and the switch-on  $T_{i+3}$  do not happen at the same time. A space  $t_m$  between these two instants is introduced in order to avoid the short circuit of the DC supply  $U_c$  during switching, it is called dead time  $t_m$ . Depending on the direction of the stator current of

the motor, the mean voltage at the terminals is written as a matrix<sup>2</sup>:

$$\begin{bmatrix} \langle v_{s1} \rangle \\ \langle v_{s2} \rangle \\ \langle v_{s3} \rangle \end{bmatrix} = \frac{U_c}{3} \begin{pmatrix} 2 & -1 & -1 \\ -1 & 2 & -1 \\ -1 & -1 & 2 \end{pmatrix} \begin{bmatrix} \lambda_{1ref} - \frac{t_m}{T_{SW}} \text{sign}(i_{s1}) \\ \lambda_{2ref} - \frac{t_m}{T_{SW}} \text{sign}(i_{s2}) \\ \lambda_{3ref} - \frac{t_m}{T_{SW}} \text{sign}(i_{s3}) \end{bmatrix} \quad (I-10)$$

The voltages obtained at the terminals of the receiver (load) for conventional three-phase inverters have several harmonics, so it is necessary to search for an approach of a sinusoidal waveform.

The block is already executed and based on the “20 sim” but cannot be used ,it does not give reliable and efficient results and the direct technique of using PWM with the inverter will lead to several errors in the simulation where r is always zero.

For this we are going to use the technique of pulse width modulation (PWM), it’s one of the two principal algorithms used in photovoltaic solar battery chargers, the other being tracking. So we will use a block between PWM and the inverter which contains (the amplitude, frequency parameters), and this called “PWM logic”. For that we represent in the following Figure 13 the model used.

In this case, the voltage and frequency outputs are controlled by the inverter using the PWM technique. For that, we represent 3 blocks for each arm and three signals of the inverter U1, U2, and U3 are obtained for respective r values r1, r2 and r3.

In fact the voltage inverter at PWM is always chosen to have a fast response and high performance.

So the Figure 14 represents the technique used already.

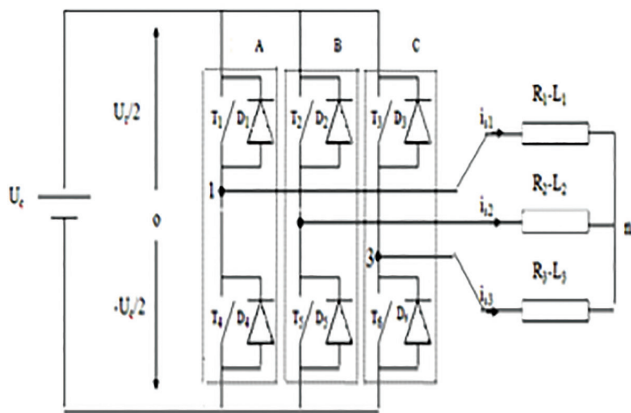


Figure 9. Diagram of the inverter and R-L load.

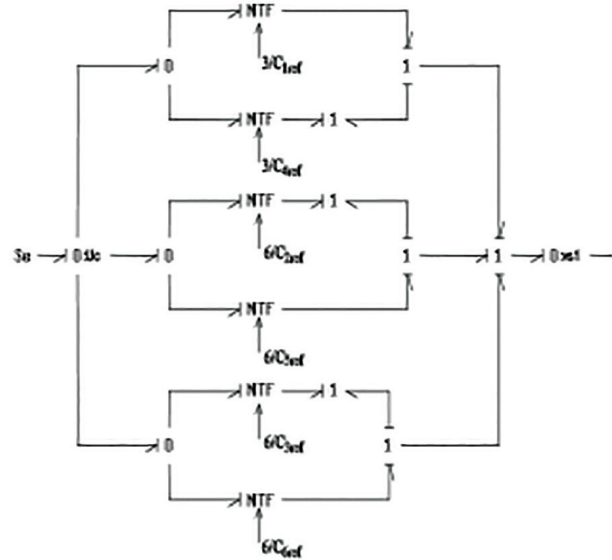


Figure 10. Sub-model bond graph of the inverter A-arm.

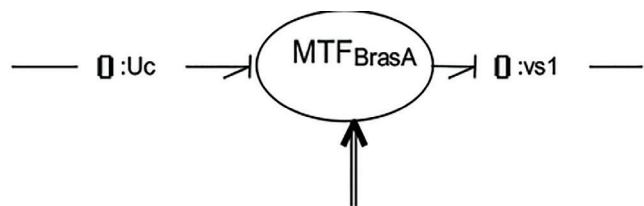


Figure 11. Bond graph model of arm A of the inverter.

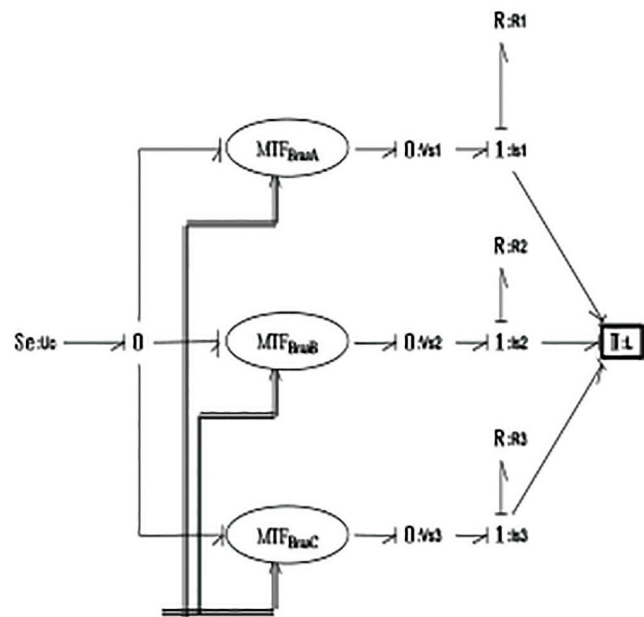


Figure 12. Bond graph model of the voltage inverter + three-phase load R-L.

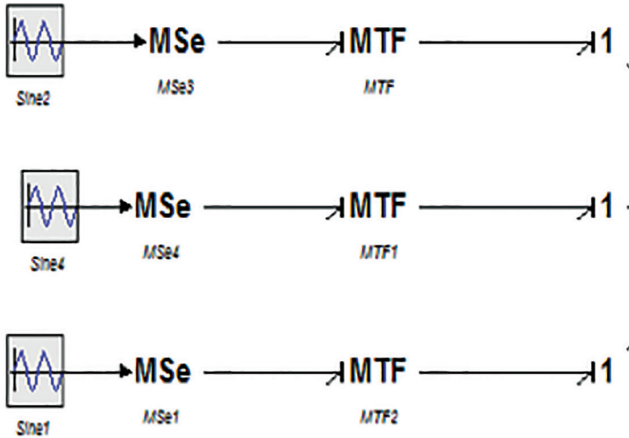


Figure 13. Bond graph model of the inverter.

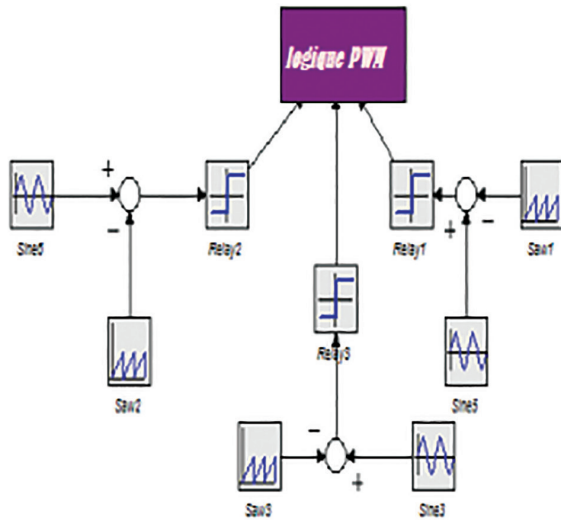


Figure 14. PWM bond graph model.

### 3. BG model of the asynchronous machine

Thanks to the development of control electronics, which allows the adjustment of speed in a very simple and effective way, all the applications using motors which foresee the possibility of speed regulation (d.c. motors or slip-ring motors) have been replaced by asynchronous motors.

The asynchronous motor is the most electrical motor used in the industry. Its main advantage is the absence of slippery electrical contacts. Thus, it has a simple, robust and easy to build structure.<sup>4</sup>

The theory of the asynchronous machine is based on the Park transformation which brings the stator and rotor electrical equations to electrically perpendicular axes

called d for the direct axis and q for the quadrature one. The asynchronous machine is modeled using the following assumptions:

- The distribution of the magnetomotive force in the air gap is sinusoidal.
- the homopolar components are zero.
- The effects of ferromagnetic losses and

Saturation are neglected.

The equation of asynchronous machine in the two-phase system (d, q) related to the rotating field are obtained using the Park

$$\begin{cases} V_{sd} = R_a I_{sd} + \frac{d\phi_{sd}}{dt} - \omega_s \phi_{sq} \\ V_{sq} = R_a I_{sq} + \frac{d\phi_{sq}}{dt} + \omega_s \phi_{sd} \\ 0 = R_r I_{rd} + \frac{d\phi_{rd}}{dt} - (\omega_s - \omega_m) \phi_{rq} \\ 0 = R_r I_{rq} + \frac{d\phi_{rq}}{dt} + (\omega_s - \omega_m) \phi_{rd} \end{cases}$$

$V_{sd}, V_{sq}$ : Stator voltage direct and quadratic.

$I_{sd}, I_{sq}$ : Stator current direct and quadratic.

$\Phi_{rd}, \Phi_{rq}$ : Direct and quadratic rotor flux.

$\omega_s, \omega_m$ : Stator and mechanical speed respectively.

There are several ways to choose the MAS state variables in the landmarks of park. In general, the choice is set by the user according to his needs in the study and design of his order. In the following case, we choose the stator currents, the rotor fluxes and the mechanical speed like state variables. In this case, the model of the asynchronous motor put into variable state form is given by several equations:

$$\frac{MR_r}{L}$$

The expression of the torque as a function of the stator currents and the rotor fluxes is given by:

$$C_{em} = P \frac{M}{L_r (\Phi_{rd} I_{sq} - \Phi_{rq} I_{sd})}$$

From the previous equations, we obtain the mode of the asynchronous motor pattern BG (dq) as illustrated in Figure 15.

About the BG modeling, there are, for the asynchronous machine, an infinity of position of the reference mark dq turning at the speed  $\theta_s = \omega_s \cdot t$ . We choose the fixed reference axis for the stator.

In this case we can write  $\theta_s = 0$ ,  $\omega_s = 0$ , this referential is named "Concordia's reference", noted  $\alpha$ - $\beta$ , the model graph of the motor is simplified as presented in Figure 16.

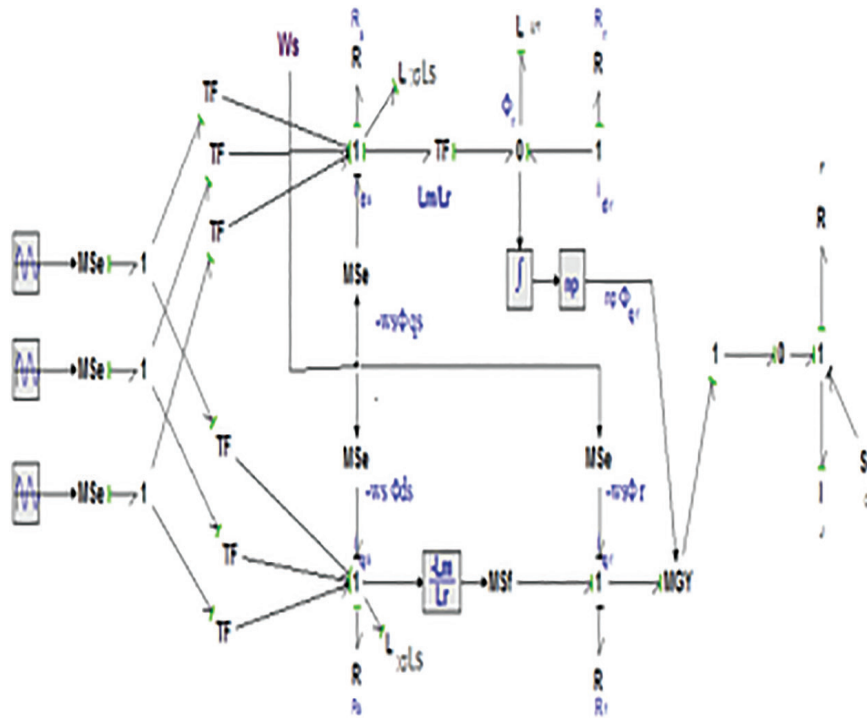


Figure 15. Model Asynchronous Motor Pattern BG (dq).

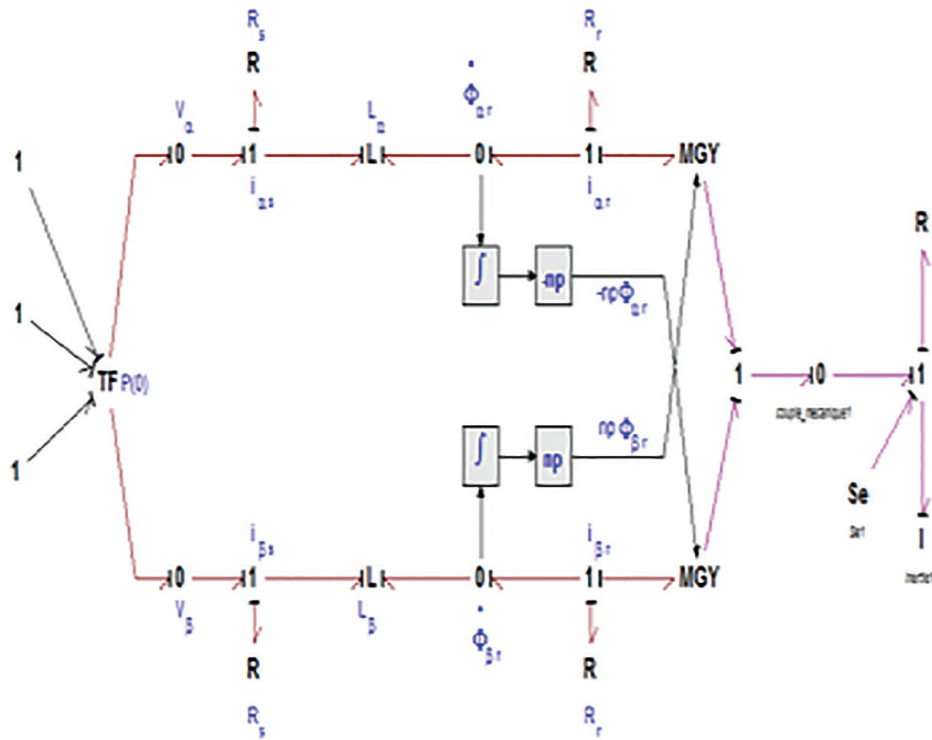


Figure 16. Asynchronous motor of bond graph in the reference.

## 4. Pump Modeling

Centrifugal pumps are a sub-class of dynamic axis-symmetric work-absorbing turbo machinery. It's a rotary machine intended to communicate to the pumped liquid a sufficient energy to cause its movement in a Hydraulic network generally comprising a geometrical height of elevation, an increase in pressure and losses of load. The fluid enters the pump impeller along or near to the rotating axis and it is accelerated by the impeller, flowing radially outward into a diffuser or volute chamber (casing), from where it exits. Common uses include water, sewage, petroleum and petrochemical pumping; a centrifugal fan is commonly used to implement a vacuum cleaner. The reverse function of the centrifugal pump is a water turbine converting potential energy of water pressure into mechanical rotational energy. Figure 17 shows the bond graph model of the centrifugal pump.

The calculation of the centrifugal pumps is carried out by dimensional analysis and by Euler's theorem<sup>2</sup>. We can define the Flow rate  $Q$  supplied by a centrifugal pump as the volume displaced during the unit of time. It is expressed in many units: cubic meters per second ( $m^3 / s$ ) or more practically in cubic meters per hour ( $m^3 / h$ ) or in liters per second ( $l / s$ ) or liters per minute ( $l / min$ ). It is called a manometric Height, from a pump  $H_{pompe}$ , the energy supplied by the pump to the unit of weight of the liquid passing through it. This height varies with the flow rate for constant speed given by the manufacturer. It is the height of a column of liquid that would determine a static pressure equal to the discharge pressure. Its expression is given by<sup>6,5</sup>.

$$H_{pompe} = b_0 \Omega_m^2 + b_1 \Omega_m Q + b_2 Q^2 \quad (I-13)$$

Where the coefficients  $b_0$ ,  $b_1$  and  $b_2$  depend on the internal geometries of the pump and are independent of the speed of rotation.

The centrifugal pump has a characteristic of the resistive torque  $C_r(\Omega)$  which is proportional to the square of its rotational speed  $\Omega_m$  and also given by the following aerodynamic equation:<sup>5</sup>

$$C_r(\Omega) = C_2 \Omega_m^2 \quad (I-14)$$

$C_2$  is the torque constant of the pump. It follows that, the useful mechanical power  $P_m$  provided by the drive motor to the pump is:

$$P_m = C_2 \Omega_m^3 \quad (I-15)$$

The mechanical losses applied to the shaft of the motor-pump unit are represented by a set of torques  $C_{fv}(\Omega)$  proportional to the speed, it is described by the following expression in which  $C_1$  is the viscous friction coefficient:

$$C_{fv} = C_1 \Omega_m \quad (I-16)$$

To the couples presented above, we can add the acceleration torque  $J d \Omega_m / dt$ ,  $J$  being the total inertness of the mechanical system and  $t$  for the time. That's why the electromagnetic torque is described by the following expression:

$$C_{em} = C_2 \Omega_m^2 + C_1 \Omega_m + J \frac{d \Omega_m}{dt} \quad (I-17)$$

The efficiency  $\eta_p$  of a pump is the ratio of the useful power  $P_{hy}$  (hydraulic power) imparted to the liquid pumped to the absorbed power  $P_{mec}$  by the pump (at the end of the shaft), the efficiency  $\eta_p$  is given by the following equation:

$$\eta_p = \frac{P_{hy}}{P_{mec}} = \frac{\rho g Q H_{pompe}}{C_2 \Omega_m^3} \quad (I-18)$$

With

$$\begin{aligned} \rho &: \text{Density: } 1000 \text{ Kg.m}^{-3} \\ g &: \text{acceleration: } 9.81 \text{ m.s}^{-2} \end{aligned}$$

In order to determinate the operating point, we use a second degree equation in  $Q$  as :

$$(b_2 - \Psi) Q^2 + b_1 \Omega_m Q + (b_0 \Omega_m^2 - H_p) = 0$$

Its resolution allows determining the flow rate of water generated by the pump for a given rotation speed

In the model,  $\Omega_{min}$  being the minimal speed from which the pump starts to generate a pumped water flow. It is given by the following relation:

$$\Omega_{min} = \sqrt{\frac{-4(b_2 - \Psi) H_p}{b_1^2 - 4(b_2 - \Psi) b_0}}$$

So, we can discuss three possible cases depending on the recorded value of the speed<sup>10</sup>:

If  $\Omega_m < \Omega_{min}$ , no rate of flow is generated by the pump, in other words:

$$Q=0$$

If  $\Omega_m = \Omega_{min}$ , the pump begins to output water corresponds to:

$$Q = Q_{min} = \frac{b_1 \Omega_{min}}{2(b_2 - \Psi)}$$

If  $\Omega_m > \Omega_{min}$ , The expression of the flow is given by:

$$Q = \frac{-b_1 \Omega_m - \sqrt{(b_1 \Omega_m)^2 - 4(b_2 - \Psi)(b_0 \Omega_m^2 - H_p)}}{2(b_2 - \Psi)} \quad (I.19)$$

With :

$b_0, b_1, b_2$  et  $\psi$  are the constant parameters.  
And  $H_p$  is the geometric height.

In the case where the tanks are constantly connected to each other and on the same plane (this is the case for our application), then we will have:

$$HP \cong 0$$

And the equation is written with the following manner :

$$Q = \left( (-b_1 - \sqrt{(b_1^2 - 4(b_2 - \Psi)(b_0 \Omega_m^2 - H_p))}) / 2(b_2 - \Psi) \right) \Omega_m = (Q_{i,nom} / (\Omega_{i,nom})) \Omega_m \quad (I-20)$$

We present the BG model of the centrifugal pump based on the equations describing the operating point of the pump. so, the model of the hydraulic network is simplified and will be given by the block diagram of Figure 18.

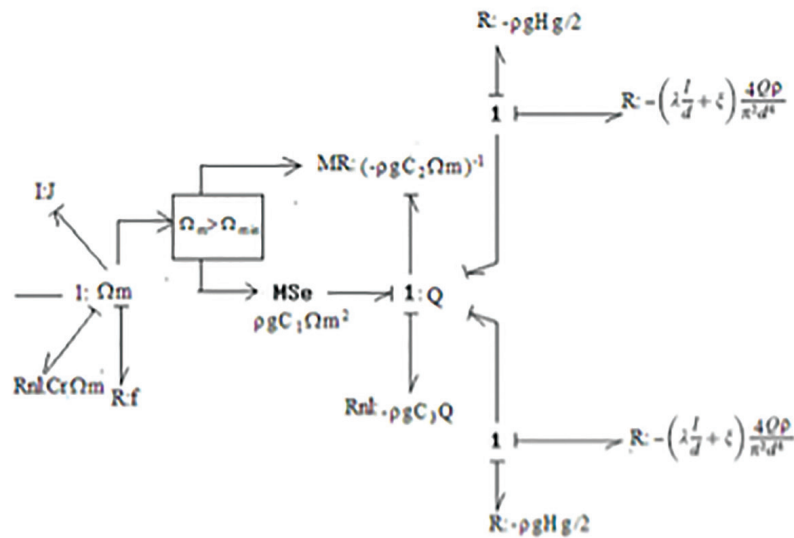


Figure 17. Bg model of the centrifugal pump.

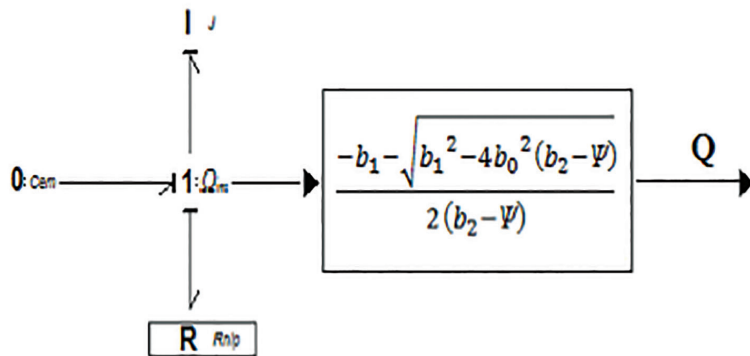


Figure 18. Modele bond graph de pompe-réseau hydraulique simplifie.

## 5. Principle of Vector Control

Vector control was introduced a long time ago. However, the appearance of the microprocessors and their computational power made it possible to apply the vector control.

It requires the calculations of Park transform, evaluation of trigonometric functions, integrations, regulations ... What could not be done in analog. The control of the asynchronous machine requires the control of torque, speed or even position. The most primary control is that of the currents and therefore the torque, it could be written directly as a function of the currents :

$$C_{em} = n_p \frac{L_m}{L_r} (\Phi_{dr} i_{qs} - \Phi_{qr} i_{ds}) \tag{I.21}$$

So, this expression is considered as a complex one. It does not draw an analogy with that of a CC machine where the natural decoupling between the adjustment of the flux and that of the torque makes its control easy; one is confronted with an additional difficulty to control this torque.

In the vector control scheme, a complex current is synthesized from two quadrature components, one of which is responsible for the flux level in the motor, and another which controls the torque production in the motor. Essentially, the control problem is reformulated to resemble the control of a DC motor. Vector control offers a number of benefits including speed control over a wide range, precise speed regulation, fast dynamic response and operation above base speed.

The main strategy is to find a law of the form  $C_{em} = K\Phi I$  which allows us to control directly the torque by ordering one of the currents ( $i_{ds}$  et  $i_{qs}$ ), it is enough to cancel one of this terms. So, if we cancel  $\Phi_{qr} = 0$  et  $\Phi_{dr} = \Phi_r$  then the couple depends only on  $i_{qs}$  and the equation become:

$$C_{em} = n_p \frac{L_m}{L_r} \Phi_r i_{qs} \tag{I.22}$$

All the previous formulas are used in the configuration of the vectorial control scheme as given in Figure 19.

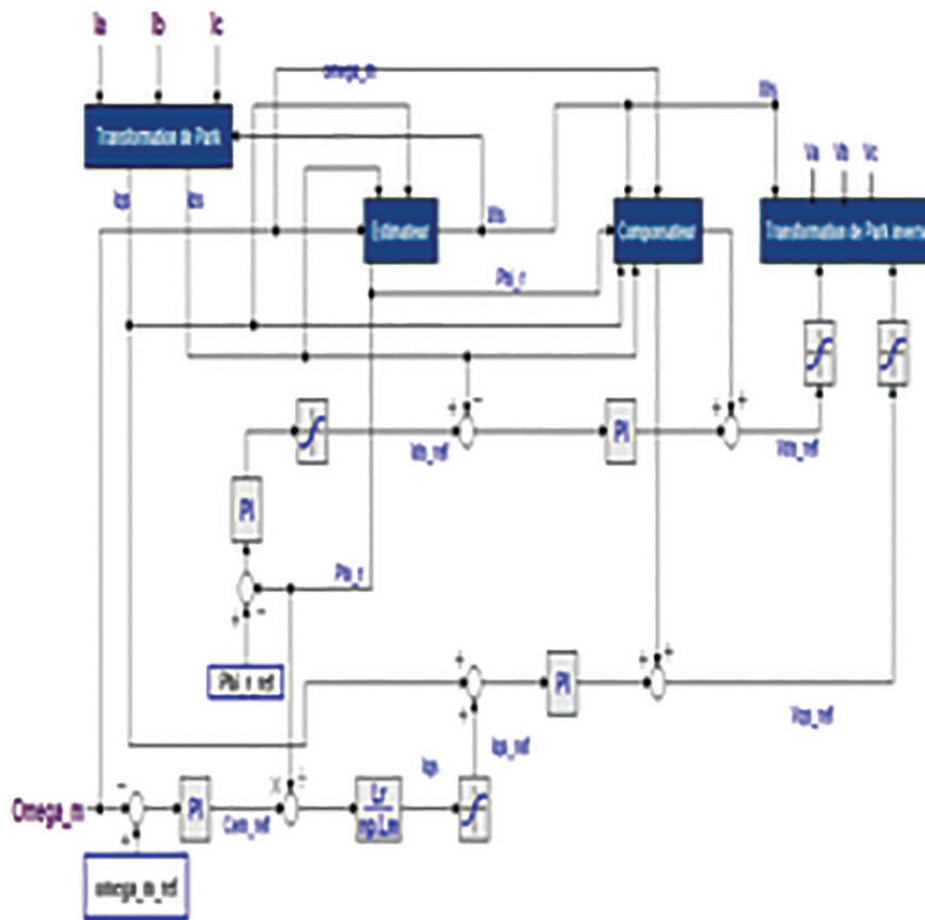


Figure 19. Scheme of the vectorial control configuration.

The different adjustments along the d axis help to impose the rotor flux while those on the q-axis make it possible to control the electromagnetic torque or the mechanical rotation speed, therefore, for a given flux, the torque can be adjusted by the unique action on  $i_{sq}$  and the motor parameters. The system of equations which determines the vector control with oriented rotor flux is given by the following equations:

$$V_{ds} = R_s i_{ds} + \sigma L_s \frac{d}{dt}(i_{ds}) - \frac{R_r L_m}{L_r^2} \Phi_{dr} - \sigma L_s \omega_s i_{qs}$$

$$V_{qs} = R_s i_{qs} + \sigma L_s \frac{d}{dt}(i_{qs}) + \frac{L_m}{L_r} n_p \Omega_m \Phi_{dr} + \sigma L_s \omega_s i_{ds}$$

The coupling terms are:

$$E_q = -\frac{R_r L_m}{L_r^2} \Phi_r - \sigma L_s \omega_s i_{qs} \tag{I.23}$$

$$E_d = \frac{L_m}{L_r} n_p \Omega_m \Phi_r + \sigma L_s \omega_s i_{ds} \tag{I.24}$$

We should have a difference in which the dynamics of the coupling terms  $E_d$  and  $E_q$  must be lower than the dynamics of the regulated quantities  $i_{sd}$  and  $i_{sq}$ , in order to compensate for the terms  $E_d$  and  $E_q$ .

So the vector control is also known as an independent or decoupled control.

### 5.1 Internal architecture of the estimator block

The estimator block allows us to act on the rotor flux and the electromagnetic torque which respectively through the components  $I_{qs}$  and  $I_{ds}$  of the stator current.

Beneficial to ensure a torque control and to be able to provide a maximum torque at any moment, the relations (I.22), (I.23) and (I.24) represent the expressions estimating the stator pulsation  $\omega_s$ , the rotor flux  $\Phi_r$  and the pair  $C_{em}$ .

The function of the stator currents  $I_{qs}$  and  $I_{ds}$  with its internal structures represented in the internal block of the estimator block shown in Figure 20.

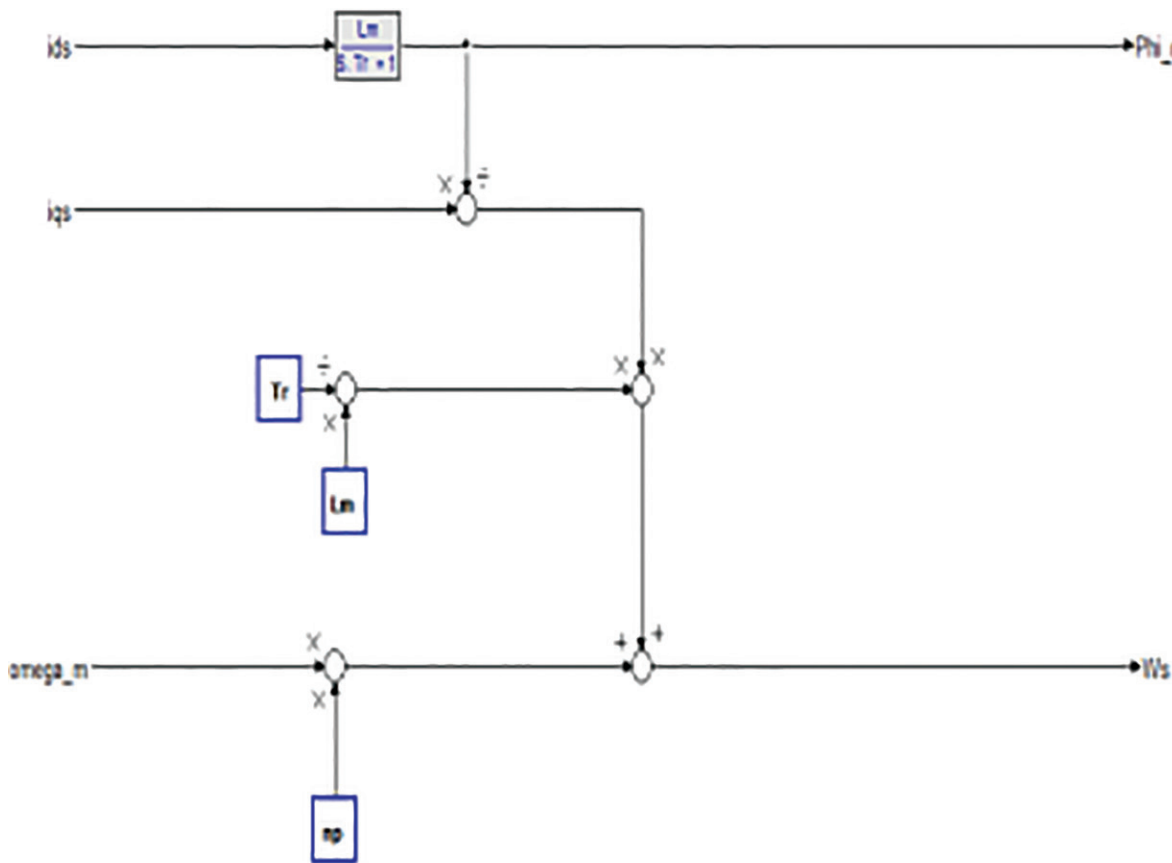


Figure 20. The internal block diagram of the estimator block.

### 5.2. Internal architecture of the compensating block

To eliminate the coupling between the two equations, we use the method of conventional compensation, which consists in decoupling the relations (I.23) and (I.24) expressing the parameters to be compensated, namely  $V_{dsc}$  and  $V_{qsc}$ , whose structure is the compensating block presented in Figure 21.

## 6. A Comparison between the Scalar and the Vector Control

The scalar control is a very simple method for controlling the speed of induction motor compared to the vector control which is more complex. Vector control is completely mathematical model on control of torque and speed of a three-phase indirect vector controlled induction motor drive.

### 6.1. Principal of Scalar Control

The scalar control is defined as an indicator of the variation control variables magnitude only and neglects the coupling effect in the machine. We can take as an example; the voltage of an induction machine can be controlled to control the flux, and frequency. Thus, flux and torque are respectively Components of frequency and voltage.

So, in the scalar method we controlled both of the magnitude and phase alignment of vector quantities.

This scalar controlled is easy to implement, but it can lead to a poor performance. But with the appearance of the vector-controlled which is demanded in many applications and by their better performance, the scalar control has diminished. Many techniques have been developed to control Alternating current (AC) power. In this application, we use the scalar control shown in Figure 22.

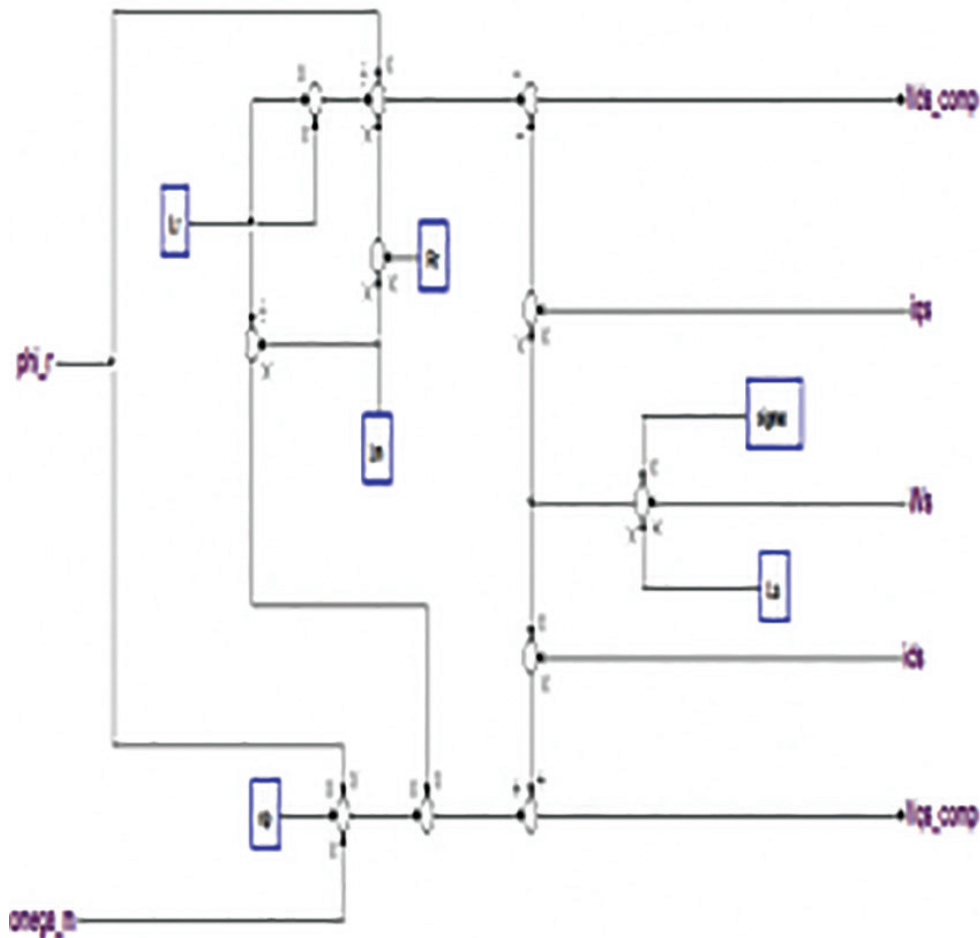


Figure 21. Internal diagram of the compensating block.

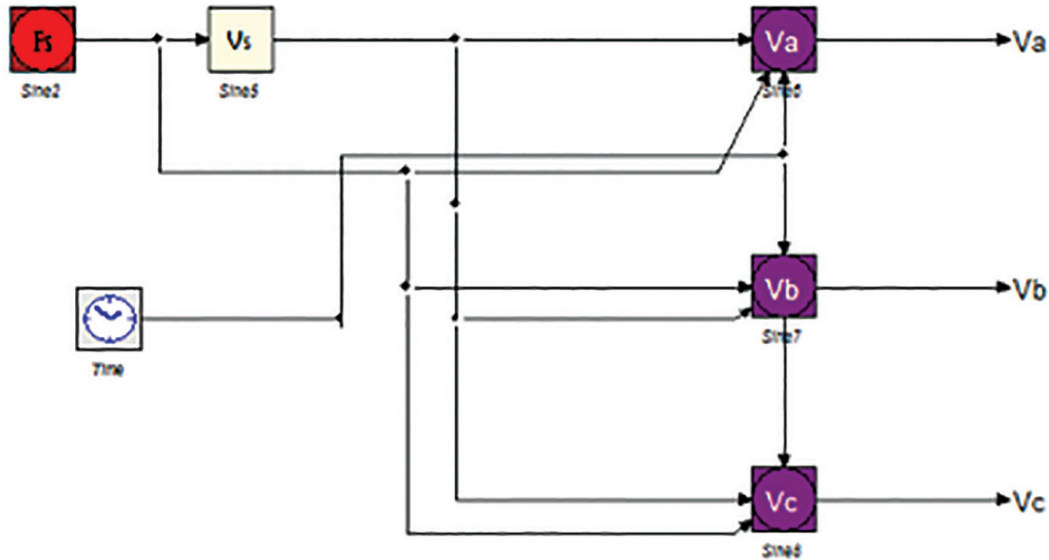


Figure 22. Scheme of the scalar control configuration.

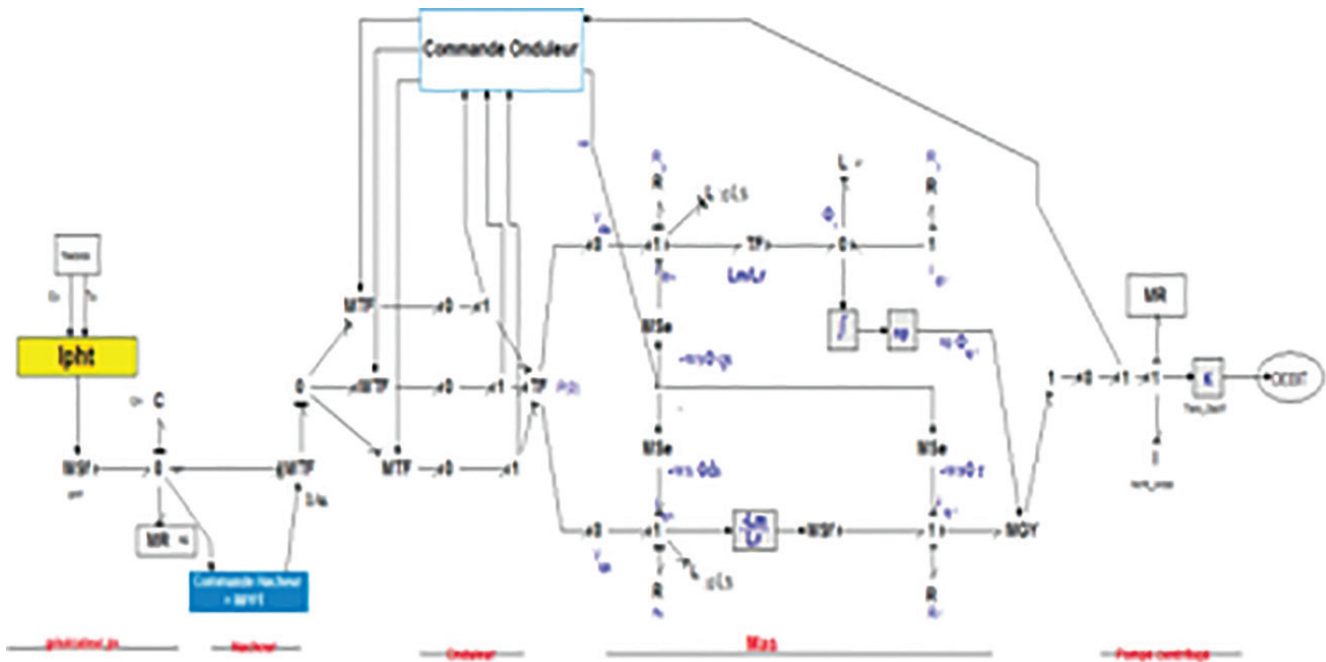


Figure 23. Simulation scheme of the photovoltaic generator powered system.

Figure 23 presents the simulation scheme of the photovoltaic generator powered system.

### 6.2 Simulation of the Closed Loop Global System

The simulation of the overall system should be used, or all control loops and the motor to be controlled are involved

in order to check whether the regulators determined in the case of isolated loops are valid or not.

We apply a step for the reference speed (300 rpm) with a nominal reference flux (0.96 Wb) after moving all the parameters in the appendix. All the simulated results are presented in Figures 24, 25, 26, 27, 28, 29.

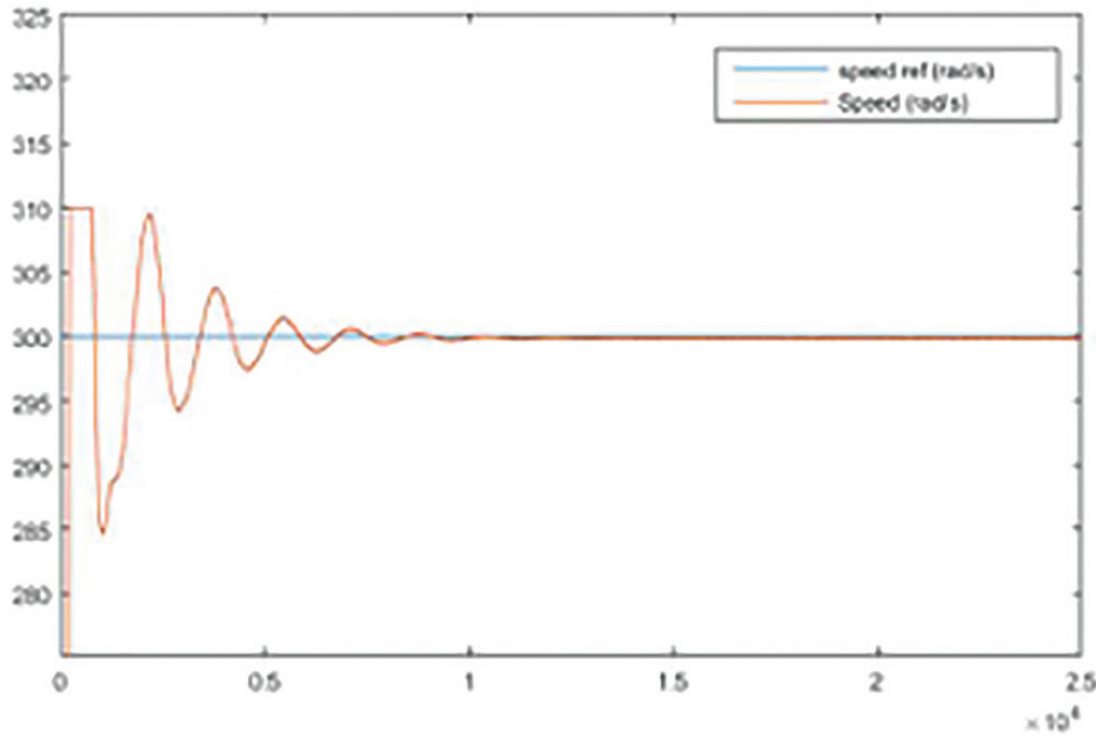


Figure 24. The speed of rotation in a closed loop.

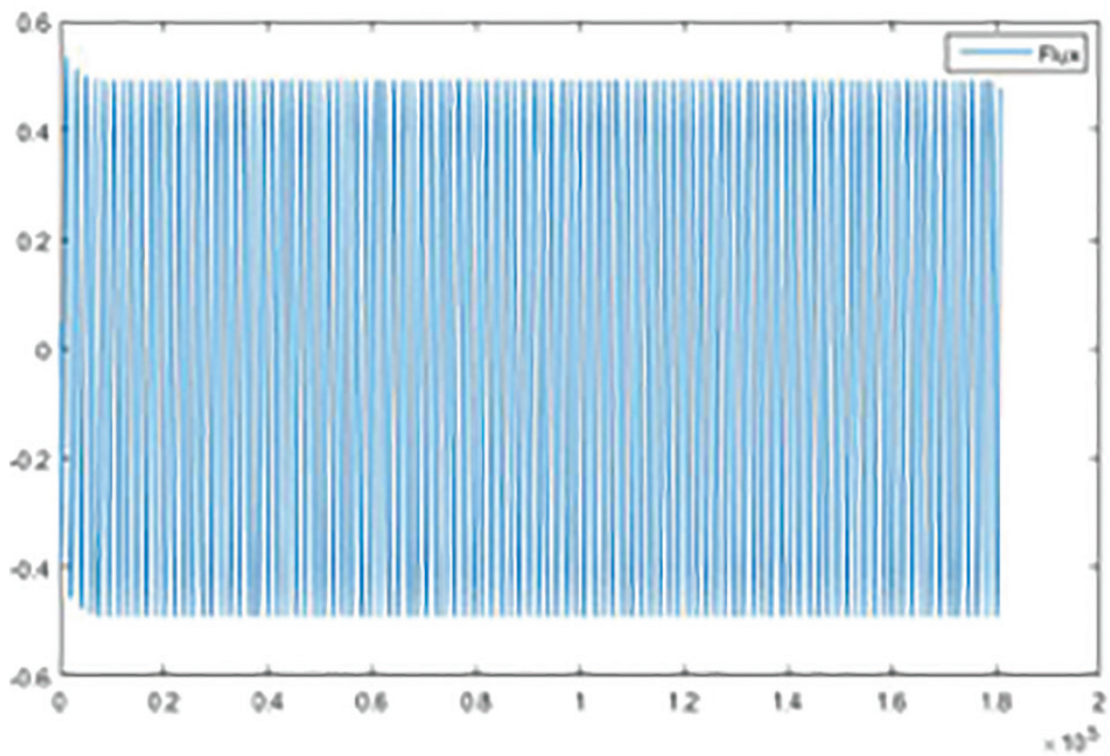


Figure 25. Speed of flow in closed loop.

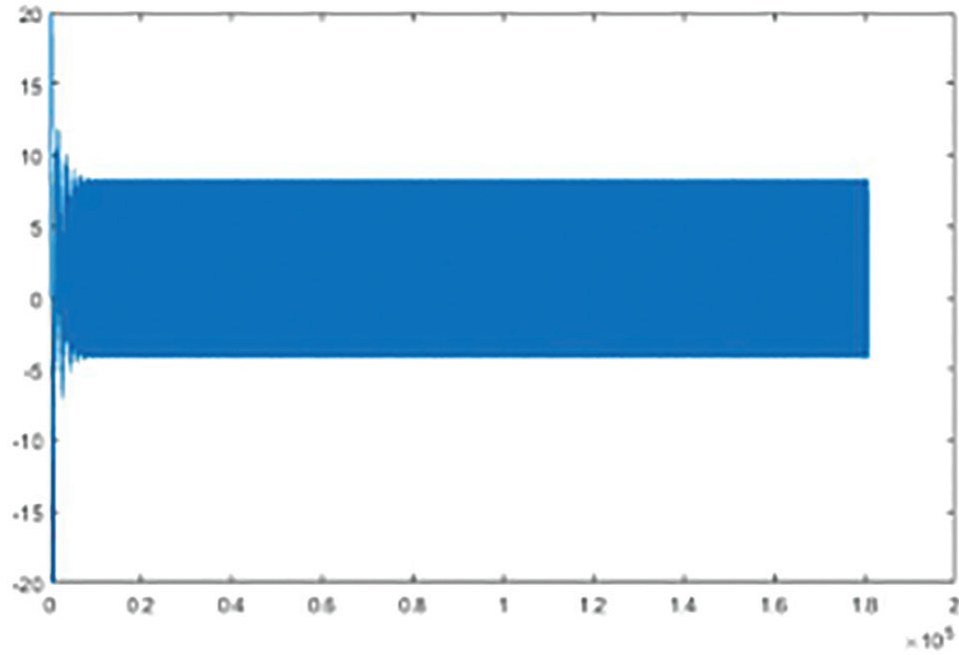


Figure 26. Speed for closed loop system.

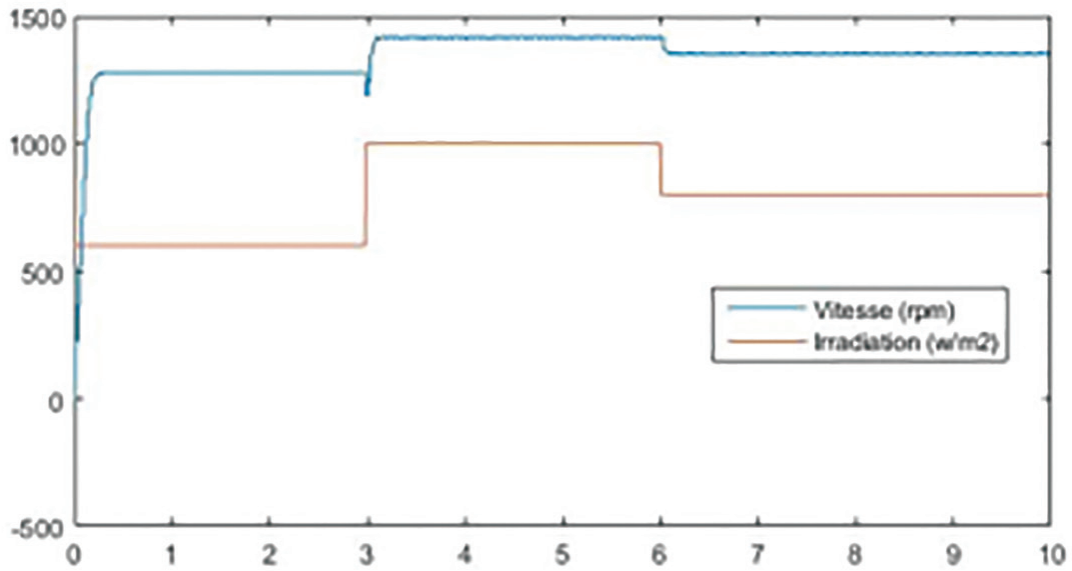


Figure 27. Time of the voltage  $V_p$  with variation of illumination.

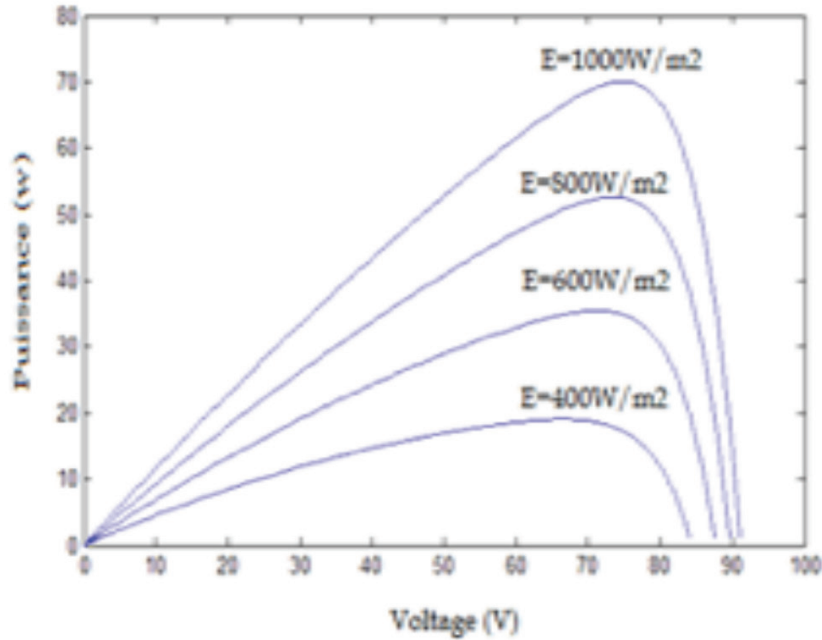


Figure 28. Power (W) for  $E_c$  variation and  $T_a = 25^\circ\text{C}$ .

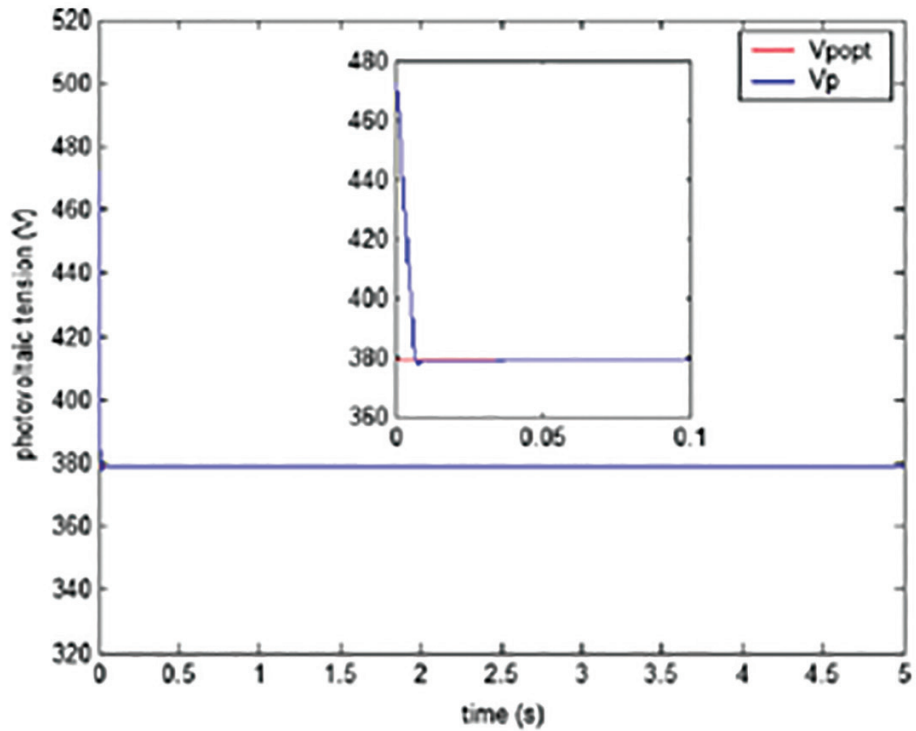


Figure 29. Simulation responses of the PV system in closed loop.

## 7. Conclusion

The work presented in this article concerns the bond graph modeling of a photovoltaic structure made up of a photovoltaic generator, a Maximum Power Point Tracking converter supplying an asynchronous motor-pump. Our use of the “20-sim” permit to study the mechanical responses of the motor-pump as well as the behavior of the photovoltaic generator. The selection and implementation of high-performance MPPT controls, there by the study and design of high-efficiency adaptation stages adapted to the constraints of solar energy.

During open loop simulation, it has been shown that the study does not ensure high performance for the asynchronous machine and the system does not respond quickly. So we proposed the control of the asynchronous closed loop machine using the principle of oriented flow: it is the theory of vector control.

## 8. Nomenclature

*BG* : Bond Graph  
*PV* : photovoltaic  
*GPV* : generator photovoltaic  
*MPPT* : Maximum Power Point Tracking  
*PWM* : Pulse Width Modulation  
*AC* : Alternating current  
*CC* : Continuous current  
*a, b, c* : Phases of the stator  
*A, B, C* : Phases of the rotor  
*d, q, h* : Direct, quadratic and homopolar axes  
*(d-q)* : Landmark of Park.  
*( $\alpha$ - $\beta$ )* : Concordia landmark.  
*T<sub>ref</sub>* : Reference ambient temperature (25 ° C or 273.15 Kelvin)  
*E<sub>cref</sub>* : Reference illumination (1000W / m2)  
*E<sub>c</sub>* : Solar illumination in W / m2,  
*T<sub>a</sub>* : Ambient temperature in ° C or Kelvin  
 $\alpha$ et  $N_p$  : In parallel association of cells and modules  
 $\beta$ et  $N_s$  : Association in series of cells and modules  
*I<sub>cci</sub>, I<sub>cc</sub>, I<sub>cct</sub>* : Short-circuit current of a diode, panel and PV generator at A  
*I<sub>ssi</sub>, I<sub>ss</sub>, I<sub>sst</sub>* : Reverse saturation currents of a diode, a panel and the PV generator in A  
*I<sub>phi</sub>, I<sub>ph</sub>, I<sub>pht</sub>* : Photocurrent of a cell, panel and PV generator in A  
*n<sub>1</sub>, n, n<sub>t</sub>* : Ideality Factor of a Diode, Panel and PV Field  
*T<sub>p</sub>* : Cell or surface temperature of GPV in ° C or Kelvin

*Q*: Charge of electrons (1.6-10-19 C)  
*K*: Boltzman constant (1.38.10-23 J / ° K)  
*Eg*: Energie of gap in Joules.  
*J* and *ji*: Current temperature constants of a cell and the PV generator  
*VTi, VT*: Thermodynamic potential of a cell and the PV generator in V  
*Vi, Vp*: Photovoltaic voltages of a cell and the PV generator in V  
*Ii, Ip*: Photovoltaic currents of a cell and the PV generator in A  
*V<sub>pop</sub>* : Reference or optimal voltage of the GPV  
*I<sub>pop</sub>* : GPV reference or optimal current  
*P<sub>pop</sub>* : Maximum power of the GPV  
*Cp*: the aerodynamic power coefficient  
 $\lambda$ : the specific speed  
 $\Omega$ : the rotational angular velocity of the turbine  
*Cem*: Electromagnetic torque (N.m)  
*I*: the inertia of the wing J  
*R*: friction of bearing f

*Ld, Lq*: respectively the direct and quadratic inductances of the stator  
*Vd, Vq*: Direct and quadratic stator voltage  
*Id, Iq*: Direct and quadratic stator voltage  
 $\Phi_e$ : the flux of permanent magnet per pole  
 $\Phi_{abc}$ : Rotor flow matrix  
 $\Phi_{rd}, \Phi_{rq}$ : Vectors of direct and quadratic flux  
 $\Phi_{sabc}$ : Stator flux matrix  
*Isd, Isq*: Vectors of direct and quadratic currents (A)  
*Lrr*: Matrix of the self-inductances and mutuals between rotor phases, (H)  
*Lss*: Matrix of clean inductances and mutuals between stator phases (H)  
*Msr*: Matrix of mutual inductances between stator and rotor phases. (H)  
*Ra*: Matrix of stator resistors  $\Omega$   
*Rr*: Matrix of rotor resistors  $\Omega$   
*Vsd, Vsq*: Vectors of direct and quadratic voltages (V)  
*U<sub>c</sub>* : Tension d'entrée de l'onduleur  
*Ci, Ti*: Control Ci of the switch Ti of the inverter (i = 1 ... 6)  
*Di*: Diode at the head in spade with the switch Ti (i = 1..6)  
*C<sub>iref</sub>*: Reference control (i = 1..6)  
*f<sub>m</sub>*: Frequency of the modulator  
*f<sub>p</sub>*: Frequency of the carrier  
*m*: Modulation index or ratio between modulating frequency and carrier frequency

$r$ : Modulation ratio or ratio between the amplitudes of modulant and carrier  
 $S$ : Control sequence of the inverter switches  
 $v_{1o}, v_{2o}, v_{3o}$ : d.d.p between lines 1, 2, 3 and the imaginary midpoint  $o$   
 $vs_1, vs_2, vs_3$ : Voltages between lines 1, 2, 3 of the inverter  
 $u_{12}, u_{13}, u_{23}$ : Single voltages of lines 1, 2, 3 of the inverter  
 $is_1, is_2, is_3$ : Currents of the lines 1, 2, 3 of the inverter  
 $\lambda_{iref}$ : Reference duty cycle ( $i = 1..3$ )  
 $n_p$ : Number of pairs of poles.  
 $\theta_m$ : Mechanical angle.  
 $\theta$ : Electrical angle between axis  $a$  and  $A$ .  
 $\theta_s$ : Electrical angle between the axes  $a$  and  $d$   
 $\theta_r$ : Electrical angle between axes  $A$  and  $d$   
 $\Omega$ : Electrical angular velocity of the d-q-h axis system.  
 $\Omega_r$ : Angular electric angular pulsation to the rotor, known as sliding.  
 $\Omega_m$ : Mechanical speed of the rotor (rd / s or rpm)  
 $\dot{\Omega}_m$ : Electrical rotation speed (rd / s)  
 $\dot{\Omega}_s$ : Pulsation of the modulant (rd / s).

## 9. References

1. Mezghanni D, Ellouze M, Cabani I, Mami A. Linearizing control of a photovoltaic structure and stability by Lyapunov directly on bond graph. *Journal of Electrical System*. 2007 Dec; 4(7):181–92.
2. Purwoadi MA. Reglage non linéaire du variateur de vitesse asynchrone sans capteur mécanique: contribution à la commande par linéarisation exacte entrées-sorties et à l'observation du flux rotorique, these de INP de Toulouse. 1996 ; 1–237.
3. Nichita C, Nichita D, Luca. Large Band Simulation of the Wind Speed for Real Time Wind Turbine Simulator. *IEEE Trans Energy Conv*. 2002 Dec; 17(4) :523–9. Crossref
4. Braustein A, Kornfeld A. Analysis of solar powered electric water pumps, solar energy. 1981; 27(3):235–40.
5. Andoulsi R, Andoulsi. Etude d'une classe de systèmes photovoltaïques par une approche bond graph. *Modelisation, analyse et commande*, Thèse UST Lille. 2001; 1–23.
6. Appelbaum J, Appelbaum. Starting and steady-state characteristic of dc motors powered by solar cell generators. *IEEE Transaction on Energy Conversion*. 1986 Mar; 1:15–25.
7. Chekireb A, Tlemcani H, Chekireb M, Boucherit. Perturb and Observe MPPT Technique Robustness Improved. *IEEE*. 2004; 845–50.
8. Tlemcani A, Chekireb H, Boucherit M. Perturb and Observe MPPT Technique Robustness Improved. *IEEE*. 2004; 845– 50.
9. Macanique des fluides. Available from: [http://www.acnancy-metz.fr/enseign/physique/PHYS/Term/Mecaflu/mecanique\\_des\\_fuides.htm](http://www.acnancy-metz.fr/enseign/physique/PHYS/Term/Mecaflu/mecanique_des_fuides.htm). Date accessed : 10/11/2005.
10. Betka A, Moussi A. Performance optimization of a photovoltaic induction motor pumping system. *Renewable Energy*. 2004; 29:2167–81. Crossref